

Chapter 6

Lattice models

Microscopic models for statistical mechanics span a broad range from detailed and complex, to idealized and simple. At one end of this range are atomistic representations of real molecules, with detailed potentials meant to represent accurately the interactions between atoms. The goal of simulations based on such models is quantitatively accurate representation of the real system in all its particular behavior. Such simulations are inevitably expensive and therefore limited. In the middle are models in which groups of atoms or entire molecules are represented by single interacting particles, with some more or less reasonable potential. Simulations based on such lumped-atom models are faster to perform, and can represent the physical behavior of the system semiquantitatively.

Lattice models are a class of microscopic models that do away entirely with the complications arising from particles moving arbitrarily in space. In a lattice model, space is represented by a regular array (lattice) of locations, with some simple degree of freedom at each location. For example, consider a lattice model of a binary mixture of two fluids A and B, in which each lattice site contains either an A or a B molecule. The degree of freedom at each site is a variable s that can take two values (say, zero if A is present, one if B is present). Interactions in such a model are typically limited to nearest neighbors.

The same lattice model interpreted slightly differently can be used to describe a single-component fluid (molecules plus vacancies), a binary fluid mixture (mixed species A and B, no vacancies), or a simple model of a magnet (array of up and down spins).

Lattice models are much simpler to simulate than “off-lattice” models of particles, because the degrees of freedom are simple, the interaction energies are easy to calculate, and the lattice sites know where to find their neighbors. Of course, we lose some fidelity to the physical system with such an idealized representation. But remarkably, lattice models do capture many essential properties of the real system, especially when those properties depend on the collective behavior of degrees of freedom over some extended region of space.

In such cases, the local details are of little consequence; what matters are larger-scale properties of the real system shared by the lattice model, such as 1) the type of degrees of freedom the lattice model contains (the “order parameter”), 2) symmetry properties (e.g., invariance under interchange of A and B in a binary mixture), 3) the type of interactions (local or long-range, “attractive” or “repulsive”), 4) the dimension of space (lattice is a line, or a plane, or a volume). Thus a properly formulated lattice model can capture the essential properties of a real system. [Exactly what constitutes a “properly formulated” lattice model, and what properties are “essential”, are topics of renormalization group analysis, well beyond the scope of these lectures.]

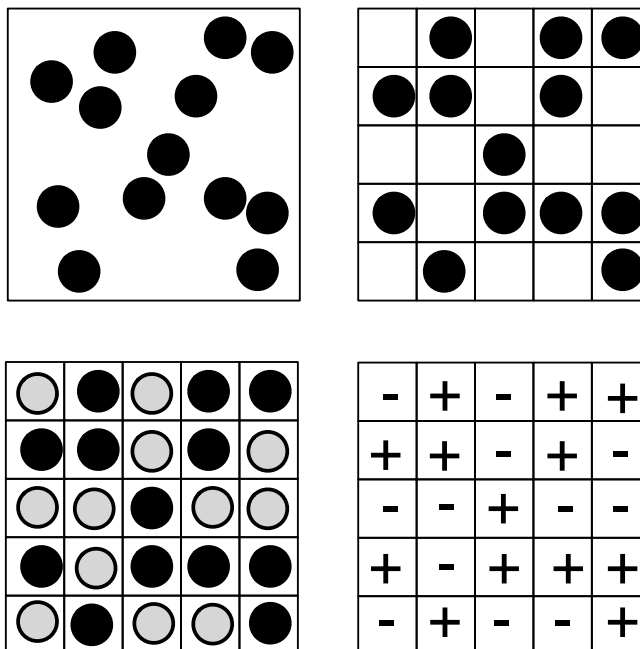


Figure 6.1: (a) Molecules in a liquid or dense gas. (b) Lattice representation of the configuration in (a). (c) Alternate view as binary mixture. (d) Alternate view as up or down (+ or -) “spins”.

6.1 Ising model

[Newman & Barkema, p. 45ff]

The simplest lattice model is the Ising model, in which each lattice site contains a single degree of freedom s that can take on two values, say ± 1 . Interactions are nearest neighbor, tending to favor adjacent lattice sites with the same value of s .

The Ising Hamiltonian can be written

$$H = -J \sum_{\text{n.n. pairs}} s_i s_j - h \sum_{\text{sites}} s_i \quad (6.1)$$

In the above, J is the interaction strength between nearest neighbors, and h is an external field coupling linearly to the sites. The cost from the first term of a “bad bond” (between sites with opposite values of s) is $2J$, relative to a completely “aligned state” (all sites with the same value of s). The field h favors “up spins” (for $h > 0$); the field energy cost of flipping a spin from up to down is $2h$.

The energy of the aligned state is $-(z/2)J$ per site, in which z is the “coordination number” of the lattice (number of bonds starting or ending on a given site). The lattice may be taken to be a variety of structures, but for our purposes we shall assume a simple square or cubic lattice in $d = 2$ or $d = 3$ dimensions respectively. For the square or cubic lattices, $z = 4$ or $z = 6$ respectively.

6.1.1 Ising model interpretations

The Ising model arises in many different physical situations. The variable s may represent an “up” or “down” magnetic moment or “spin” in a simple model of a magnetic material, in which nearby spins tend to align with each other, and are coupled to an externally applied magnetic field h .

We may also interpret s as related to the occupation of a lattice site by one of two different species A and B in a fluid binary mixture. In $d = 2$ dimensions, the two species A and B may be interpreted as “occupied” and “nonoccupied” sites in a model of molecules adsorbed to a surface.

The Ising model can be cast in a variety of equivalent forms. For problems in which we interpret the site variable as related to the occupation of site i by some species, we prefer to define a site variable $\sigma_i = (1 + s_i)/2$ that takes on the values 0 (unoccupied) or 1 (occupied).

Then the Hamiltonian can be written as

$$\begin{aligned} H &= \chi \sum_{\text{n.n. pairs}} (\sigma_i(1 - \sigma_j) + (1 - \sigma_i)\sigma_j) - \mu \sum_{\text{sites}} \sigma_i \\ &= -(\chi/2) \sum_{\text{n.n. pairs}} s_i s_j - (\mu/2) \sum_{\text{sites}} s_i + (\chi z/2 - \mu/2)N \end{aligned} \quad (6.2)$$

The first term imposes a cost of χ for a “bad bond” (adjacent sites occupied with different species), relative to a state in which all sites are occupied with the same species. Likewise, the second term imposes a bias towards occupied states (for $\mu > 0$). The cost of changing a single site from $\sigma = 1$ (occupied) to $\sigma = 0$ (unoccupied) is simply μ .

The “occupation” Hamiltonian is equivalent to the Ising Hamiltonian, as can be seen by substituting $\sigma_i = (1 + s_i)/2$ and rearranging, to obtain the second line in Eq. (6.2). (Here z is the number of neighbors per site, and N the number of sites in the lattice). With $\chi = 2J$ and $\mu = 2h$, the two Hamiltonians are the same up to a constant shift $(\chi z/2 - \mu/2)$ of the energy per site.

The Ising model can be generalized in many ways; one interesting generalization is to let the site variable take on $p > 2$ different values instead of just two values (+1 and -1 for spins, or 0 and 1 for occupation). We may think of this as corresponding to a lattice occupied by p different species.

Of course, this invites the question of how these p species should interact, which in general involves $p(p - 1)/2$ different interaction energies, even for near-neighbor interactions. The simplest model would be to assume that each pair of adjacent sites occupied by different species has the same energy cost J , no matter what different species are present.

This is the p -state Potts model, with Hamiltonian

$$H = J \sum_{\text{n.n. sites}} (1 - \delta_{s_i s_j}) - b \sum_{\text{sites}} \delta_{s_i 0} \quad (6.3)$$

in which the s_i take on p distinct values, say $0, 1, \dots, p - 1$. The cost of a bad bond is J , relative to an aligned state (all s_i the same value). For $p = 2$ we recover the Ising model, written in yet another equivalent form.

6.1.2 MC for lattice models

To simulate a lattice model with Monte Carlo using the Metropolis method, we need to specify a set of proposed moves. The simplest move for a lattice model is to choose a site at random, and then to change its site variable from its present value to one of the other possible values, chosen at random. For the Ising model, this amounts to trying to “flip” a randomly chosen “spin”.

This prescription will evidently satisfy detailed balance; any spin is equally likely to be chosen to flip, and any target value is equally likely to be chosen, so that the attempt rates to and from microstates r and s connected by a single spin flip are clearly equal.

Note that single spin flips do not conserve the quantity of each species present. We are sometimes interested in simulations in which the number of each species is conserved. We may either be

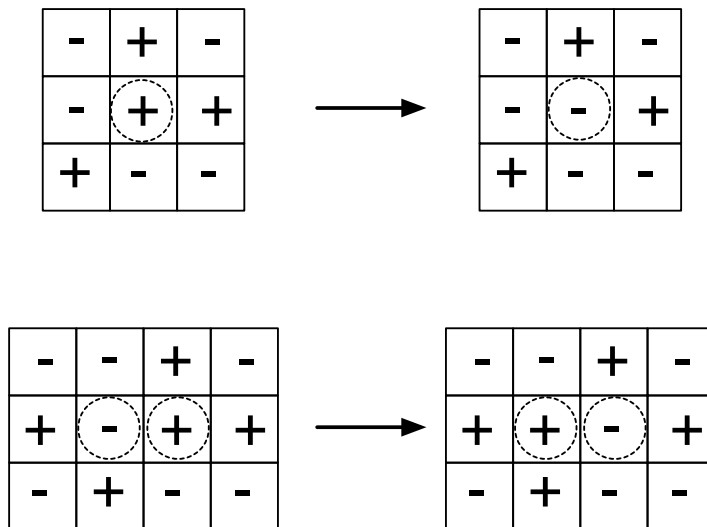


Figure 6.2: Top: single spin flip. Bottom: exchange of neighboring spins, conserving total spin.

concerned with an equilibrium problem in which the relevant ensemble is one in which the total number of some species is conserved, such as the shape of a droplet of one component surrounded by another.

In such cases, instead of single spin flips, we can construct Monte Carlo moves in which pairs of spins are exchanged. If we are only interested in preserving the total number of spins, but not representing the time-dependence of how spins move around, we can exchange distant pairs of spins, which evidently samples configuration space faster than obliging spins to diffuse.

Alternatively, we may actually be interested in representing the dynamical behavior of the simulation, i.e., we may want the spins to diffuse locally. In such a case, we can construct Monte Carlo moves in which pairs of adjacent spins are exchanged. This local spin-exchange dynamics (called Kawasaki dynamics) will be faithful to the conservation law, but will be much slower to explore the equilibrium ensemble than either spin flip or nonlocal spin exchange Monte Carlo. The equilibrium ensemble contains microstates with local variations in the concentration of species; to get from one such state to another in which the variations are unrelated, under spin-exchange dynamics the excess in species must diffuse across the region. If the regions are large (as near a critical point, see below) this process is very slow. We shall discuss local and nonlocal spin exchange Monte Carlo further below.

6.2 Mean-field theory

Very few systems are simple enough that we can evaluate their partition functions exactly. Essentially, only those systems that can be thought of as a set of noninteracting degrees of freedom (particles in an ideal gas, or independent spins on a lattice, or independent modes of oscillation in a harmonic solid) are simple enough for an exact calculation of the partition function.

For the vast majority of systems, we need approximate methods for computing the partition function. Simulations provide one approach, in which we contrive to generate a large set of microstates that are representative of the desired ensemble; averaging numerically over the microstates allows us to perform ensemble averages on a computer. While extremely useful, this approach does not of course give any analytical results.

Here, we present a broadly applicable analytical approximation to the partition function, called mean field theory. Mean field theory can be introduced and derived in many ways. In essence, it represents an instance of Polya's dictum for solving hard problems:

If you can't solve a problem, then there is an easier problem you can solve: find it.

Here, the hard problem we cannot solve is computing the partition function for many interacting entities; the easier problem we can solve is computing the partition function for a single degree of freedom in a "mean field" that represents the average influence of all the other entities in the system.

An intuitive argument for a mean-field approximation to the lattice free energy can be given quite simply, as follows. The Helmholtz free energy F is quite generally equal to $\bar{E} - TS$. For a nontrivial interacting system such as the Ising model, there is no easy analytical calculation for either the average energy \bar{E} or the entropy S . However, we can give a simple estimate of both quantities, by assuming that the typical microstates of a homogeneous phase are completely randomly mixed.

This is a reasonable assumption at high temperatures, but certainly not accurate at lower temperatures, where the two mixed species begin to be correlated in their locations, with A molecules tending to be located next to other A molecules, so as to avoid at least some unfavorable A-B contacts. These correlations evidently reduce the entropy, relative to completely random mixing of the two species.

Nevertheless, we can estimate the average energy \bar{E} assuming random mixing by replacing all appearances of σ_i in Eq. 6.2 with its average value ϕ , to obtain an estimate of the average energy per site as

$$\bar{E}/N \approx \chi z \phi (1 - \phi) \quad (6.4)$$

Here N is the total number of lattice sites and z is the number of neighbors per site. Each site "owns" $z/2$ bonds, each of which is a "bad bond" with probability $2\phi(1 - \phi)$. (In the above, we have dispensed with the chemical potential term, which we may colloquially say was present only to enforce the desired average value of ϕ .)

Correspondingly, we can estimate the entropy per site S/N by saying that the occupation of each site is chosen independently of other sites (random mixing again), with probability ϕ to be species A and $1 - \phi$ to be species B. Using the information-theoretic entropy from Section 2.4.3, we have

$$S/(kN) \approx -\phi \log \phi - (1 - \phi) \log(1 - \phi) \quad (6.5)$$

This expression can be obtained as well by elementary counting arguments. The number of ways Ω of placing n_A molecules of species A and n_B of species B on a lattice with N sites and no

vacancies (i.e., $N = n_A + n_B$) is simply given by

$$\Omega = \binom{N}{n_A} = \frac{N!}{n_A!n_B!} \quad (6.6)$$

The entropy S is $k \log \Omega$; using the simplest form of the Stirling formula, we soon obtain Eq. (6.5), with $\phi = n_A/N$ and $1 - \phi = n_B/N$.

We note in passing that if of the species (A, say) is dilute in the other, S becomes

$$S/(kN) \approx -\phi \log \phi + \phi \approx -\phi \log \phi \quad (6.7)$$

which is the lattice entropy of a dilute ideal gas (the last term being the leading contribution for small ϕ).

Putting together Eqs. (6.4) and (6.5) as $\bar{E} - TS$, we have finally

$$F/N \approx z\chi\phi(1 - \phi) + kT [\phi \log \phi + (1 - \phi) \log(1 - \phi)] \quad (6.8)$$

which is certainly a manageable (and thus popular) approximate free energy. This expression is called a mean-field approximation, for reasons that will become clear in the next section. The approximate free energy is symmetric under interchange of ϕ and $1 - \phi$, which corresponds to exchange of the species labels A and B. The two terms in Eq. (6.8) approximate the energy and entropy per site, and favor demixing and mixing respectively. The first term is concave down in ϕ , the second concave up; the second term favors a minimum at $\phi = 1/2$ (mixed state), while the first term struggles against such a mixed state.

One question that immediately arises: how good an approximation is this to the true free energy? We can immediately observe that the approximations for both E and S are overestimates. The energy assuming random mixing ignores how correlations can avoid repulsive interactions, and the entropy assuming random mixing assumes all site occupations can be chosen independently — which they cannot, if the system is correlated to avoid repulsive interactions. We may hope that because F is the difference $E - TS$, that fortune may favor us with canceling errors in E and S . In the next section, we shall show that this free energy is in fact an upper bound to the true free energy.

6.2.1 Variational theorem

We relate the easy (mean-field) problem to the hard (exact) problem with the aid of a variational theorem, which states that the true free energy F is lower than any estimate F_{est} we can make based on a model partition function:

$$F \leq F_{est} \equiv \langle H \rangle_0 - TS_0 \quad (6.9)$$

Here the subscript 0 refers to a “model” partition function, in which the actual energies E_r and microstate probabilities $P_r = e^{-\beta E_r}/Z$ are replaced by a more convenient set of model microstate energies $E_{r,0}$ and probabilities $P_{r,0}$, defined by

$$\begin{aligned} P_{r,0} &= \frac{e^{-\beta E_{r,0}}}{Z_0} \\ Z_0 &= \sum_r e^{-\beta E_{r,0}} = e^{-\beta F_0} \end{aligned} \quad (6.10)$$

The entropy of the model partition function is S_0 .

The model free energy F_0 can be written $E_0 - TS_0$, in which E_0 is the average model energy in the model ensemble, given by $\langle H_0 \rangle_0$. Using this, we can rewrite the estimated free energy F_{est} in an alternate form as

$$F_{est} = F_0 + \langle H - H_0 \rangle_0 \quad (6.11)$$

The point of the theorem (which we shall prove below) is that any model partition function provides an upper bound to the free energy. In practice, we choose the microstate energies $E_r^{(0)}$ in some convenient way, so that we can evaluate the model partition function exactly, while at the same time providing some reasonable approximation to the physics of the system.

Most commonly, the model partition function involves approximating a system of many interacting particles or molecules with a system in which each particle or molecule interacts with the others only through some mean field, such as the average concentration. We shall introduce such a mean-field approximation in the next section.

We now set about proving the theorem. We will show that the right-hand side, when minimized over the choice of weights P_{r0} , gives the left hand side, with P_{r0} equal to the actual microstate probabilities P_r . (The discussion here is closely related to the arguments given in Section 2.4.3 that maximizing the information-theoretic entropy subject to the constraint of fixed average energy leads to the canonical ensemble.)

We begin by expressing F_{est} in terms of P_{r0} , using the result Eq. (??) for the information-theoretic entropy of the model ensemble to write

$$F_{est} = \sum_r E_r P_{r0} + kT \sum_r P_{r0} \log P_{r0} \quad (6.12)$$

Now we minimize the above with respect to P_{r0} subject to the normalization constraint on P_{r0} , using the method of Lagrange multipliers. [This we do by minimizing $\beta F_{est} - \lambda(\sum_r P_{r0} - 1)$.] We find

$$0 = \beta E_r + \log P_{r0} + 1 - \lambda \quad (6.13)$$

Solving for P_{r0} and imposing normalization (which determines λ), we find the optimum value P_{r0}^* is the true microstate probability,

$$P_{r0}^* = \frac{e^{-\beta E_r}}{\sum_r e^{-\beta E_r}} = P_r \quad (6.14)$$

We can verify that this is a minimum, by expanding F_{est} to second order around the optimum values P_{r0}^* . The second order correction is

$$\Delta F_{est} = (1/2) \sum_{r,r'} \frac{\partial^2 F_{est}}{\partial P_{r0} \partial P_{r'0}} (P_{r0} - P_{r0}^*) (P_{r'0} - P_{r'0}^*) \quad (6.15)$$

The only contribution to the second derivative matrix comes from the terms $kT \sum_r P_r \log P_r$, so that we have

$$\frac{\partial^2 F_{est}}{\partial P_{r0} \partial P_{r'0}} = \frac{kT}{P_{r0}^*} \delta_{r,r'} \quad (6.16)$$

which is evidently a diagonal matrix, with all positive terms. Thus the second-order corrections to F_{est} when we shift away from P_{r0}^* are guaranteed to be positive, and the extremum we have found is a minimum.

6.2.2 Bragg-Williams approximation

We make use of the variational theorem of the previous section, to derive a mean-field theory for a binary mixture described by the “occupation” form of the Ising Hamiltonian. We write our model Hamiltonian as a system of single spins interacting only with an effective chemical μ_m :

$$H_0 = -\mu_m \sum_i \sigma_i \quad (6.17)$$

The strength of μ_m will be determined by minimizing the mean-field free energy estimate, given by the right-hand side of the variational theorem.

In the present problem, the number of particles present fluctuates, while the chemical potential μ is fixed; hence we write the mean-field free energy as A_m , corresponding to its status as a grand canonical potential.

It turns out to be more convenient to work in terms of the average site fraction $\phi(\mu_m)$, given by the average of the local site occupation variable σ_i in the model ensemble, which takes on values zero or one.

$$\phi = \langle \sigma \rangle_0 \quad (6.18)$$

This average in the model ensemble is simple to evaluate, because each occupation variable interacts only with μ_m ; we have

$$\phi = \frac{e^{\beta\mu_m}}{e^{\beta\mu_m} + 1} = (1/2)(1 + \tanh(\beta\mu_m/2)) \quad (6.19)$$

We may think of μ_m in turn as a function of the true μ , since the value of μ_m on minimizing A_m will depend on μ .

The model ensemble entropy is simple to evaluate, because the site occupation variables σ_i are all independently varying. Since the probability of any σ_i being equal to 1 is ϕ , we can write the model entropy S_0 as

$$\begin{aligned} S_0 &= -N \sum_r P_r \log P_r \\ &= -N (\phi \log \phi + (1 - \phi) \log(1 - \phi)) \end{aligned} \quad (6.20)$$

Likewise, the average of the true Hamiltonian in the model ensemble is easily evaluated, because the value of each occupation variable varies independently. The average $\langle H \rangle_0$ can be expressed in terms of ϕ as

$$\langle H \rangle_0 = z\chi\phi(1 - \phi) - \mu\phi \quad (6.21)$$

The combined right-hand side is the model grand canonical free energy A_m , given by

$$\begin{aligned} A_m/N &= z\chi\phi(1 - \phi) + T(\phi \log \phi + (1 - \phi) \log(1 - \phi)) - \mu\phi \\ &\equiv F_m(\phi)/N - \mu\phi \end{aligned} \quad (6.22)$$

This form of $F_m(\phi)$ is the Bragg-Williams approximation, which we informally wrote down at the beginning of this section.

Minimizing with respect to μ_m , which indirectly controls the value of ϕ in the model ensemble, leads to

$$\begin{aligned} 0 &= \frac{\partial}{\partial \mu_m} (F_m(\phi)/N - \mu\phi) \\ &= \frac{\partial F_m/N}{\partial \phi} \frac{\partial \phi}{\partial \mu_m} - \mu \frac{\partial \phi}{\partial \mu_m} \end{aligned} \quad (6.23)$$

which evidently results in

$$\frac{\partial F_m/N}{\partial \phi} = \mu \quad (6.24)$$

6.2.3 Legendre transform

This is the same relationship that holds for the true grand canonical free energy $A(h)$, defined via Legendre transform from the Helmholtz free energy $F(\phi)$ as

$$A(\mu) = F(n) - \mu n \quad (6.25)$$

with $\phi = n/N$ (n the number of occupied sites, N the total number of sites). Standard thermodynamic derivatives give $\mu = \partial F/\partial n$, and so

$$\mu = \frac{\partial F/N}{\partial \phi} \quad (6.26)$$

consistent with the results of the previous section.

We recall from Section 2.4 that the Legendre transform arises when we change ensembles. We start with a partition function in which we sum over microstates at fixed total number of sites of each species,

$$Z = e^{-\beta F} = \sum_r e^{-\beta H} \quad (6.27)$$

To relax the constraint of fixed total number of occupied sites, we introduce a field μ that couples to the operator $\sum_i \sigma_i$, and extend the sum over microstates to include states with different total number of occupied sites,

$$Z_g = e^{-\beta A} = \sum_r e^{-\beta(H - \mu \sum_i \sigma_i)} \quad (6.28)$$

Evidently we have

$$\phi = \frac{1}{N} \left\langle \sum_i \sigma_i \right\rangle = -\frac{\partial A/N}{\partial \mu} \quad (6.29)$$

The connection between the two thermodynamic potentials arises as in Section 2.4 from approximating the extended partition sum with its dominant terms, that correspond to the most likely value of ϕ , so that

$$Z_g \approx Z e^{\beta \mu N \phi} \quad (6.30)$$

This leads to

$$A(\mu) = F(\phi) - \mu N \phi \quad (6.31)$$

which is the same relation for the true potentials as holds for the model potentials.

6.3 Mean-field phase behavior

As the strength of the repulsive interaction χ between unlike species A and B is increased, a binary mixture will ultimately cross a phase boundary, and demix into coexisting A-rich and B-rich phases. The shape of $f(\phi)$ determines the phase behavior of a binary mixture.

For symmetric binary mixture, invariant under interchange of A and B, $f(\phi)$ is symmetric about $\phi = 1/2$. Note that the function $f(\phi)$ is the sum of a concave down function (the repulsive energy) and a concave up function (the entropy). At high temperatures, the entropy dominates, and $f(\phi)$ has a single minimum at $\phi = 1/2$.

As the temperature is reduced, the repulsive energy becomes more important, and $f(\phi)$ develops a pair of minima of equal depth, symmetrically displaced from $\phi = 1/2$. The dimensionless quantity $\beta\chi$ measures the relative importance of the repulsive energy between unlike species, and the configurational entropy of a random mixture of two species.

6.3.1 Coexistence

In Section 2.5.2, we showed directly from the grand canonical ensemble that one form of the conditions for coexisting phases are equal temperatures, chemical potentials, and equal minimum values of the grand potential A .

From the Legendre transform relations, the slope of the function $F(\phi)/N$ (henceforth written $f(\phi)$) is the chemical potential μ . For some ranges of μ , there is only a single value of ϕ at which $f'(\phi) = \mu$, and hence only one possible phase for this value of μ . But when the function $f(\phi)$ is not everywhere convex, there will be some values of μ for which there are multiple values of ϕ at which $\partial f(\phi)/\partial\phi$ equals μ .

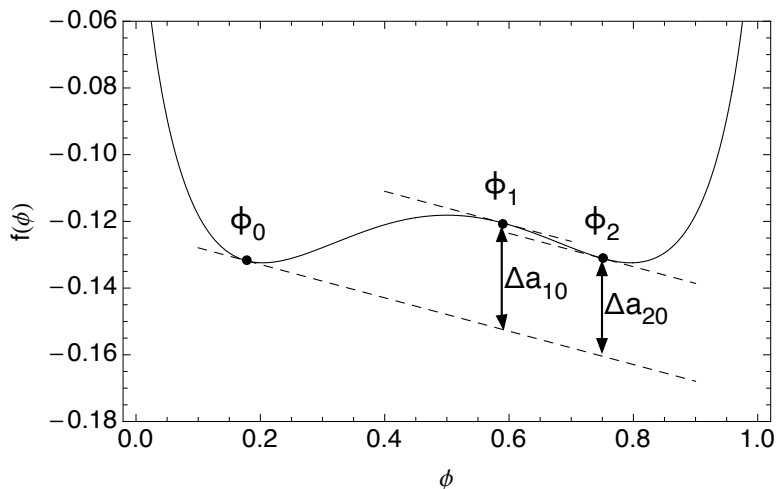


Figure 6.3: Free energy curve $f(\phi)$ in Bragg-Williams approximation for symmetric binary mixture at $\beta\chi = 2.3$, with tangency points ϕ_0, ϕ_1, ϕ_2 for $\mu = -0.05$. Both Δa_{10} and Δa_{20} are positive; ϕ_0 is equilibrium phase.

Now consider the line $t(\phi; \phi_0)$ tangent to the curve $f(\phi)$ at ϕ_0 . The equation for this line is $t(\phi; \phi_0) = f(\phi_0) + \mu_0(\phi - \phi_0)$, where μ_0 equals $f'(\phi_0)$. The vertical distance $d(\phi; \phi_0)$ from the curve $f(\phi)$ to this tangent line can be written

$$d(\phi; \phi_0) = f(\phi) - (f(\phi_0) + \mu_0(\phi - \phi_0)) \quad (6.32)$$

The Legendre transform tells us that $A(\mu)/N$ (henceforth $a(\mu)$) is equal to $f(\phi) - \mu\phi$, with $\mu = f'(\phi)$. Suppose there are two points ϕ_0 and ϕ_1 on $f(\phi)$ with the same slope. We can find which has the smallest value of A , by taking the difference

$$\begin{aligned} a(\phi_1) - a(\phi_0) &= (f(\phi_1) - \mu_0\phi_1) - (f(\phi_0) - \mu_0\phi_0) \\ &= f(\phi_1) - (f(\phi_0) + \mu_0(\phi_1 - \phi_0)) = d(\phi_1; \phi_0) \end{aligned} \quad (6.33)$$

But this is simply the vertical distance from the curve $f(\phi)$ at ϕ_1 , down to the tangent line $t(\phi; \phi_0)$.

So if the point on the curve $f(\phi_1)$ lies above the tangent line through ϕ_0 , the state at ϕ_0 has lower grand potential, and corresponds to the equilibrium phase. Whereas, if the point on the curve $f(\phi_1)$ lies *on* the tangent line, the states at ϕ_0 and ϕ_1 have the same value of grand potential (and the same chemical potential μ , and temperature). Thus the conditions for coexisting phases are fulfilled, and the states at ϕ_0 and ϕ_1 represent coexisting phases.

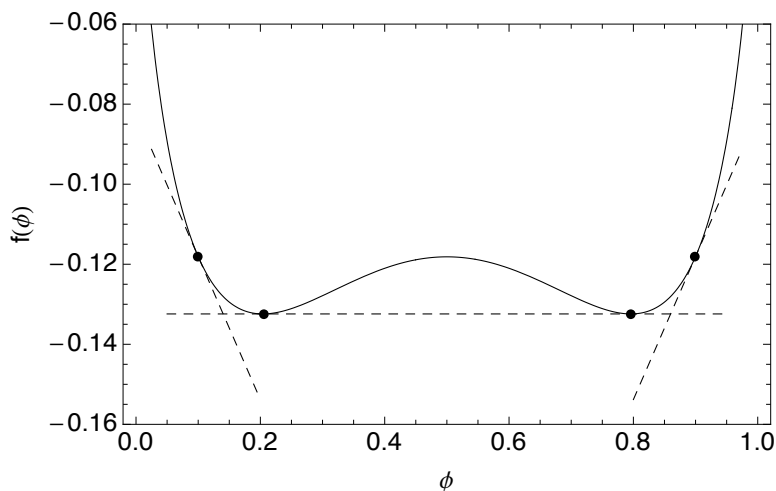


Figure 6.4: Free energy curve $f(\phi)$ in Bragg-Williams approximation for symmetric binary mixture at $\beta\chi = 2.3$, with two tangents corresponding to single phases, and one common tangent corresponding to two coexisting phases.

This graphical recipe for finding coexisting phases is called the common tangent construction. We can find the single or coexisting phases for $f(\phi)$ by “rocking” a tangent along the outside of the curve. The tangency point is the value of ϕ for the given μ value.

When we encounter a curve $f(\phi)$ which is not entirely convex — for example, which takes the form of a double well potential, as does our model $f(\phi)$ for a symmetric binary mixture — we discover that a portion of the curve (between the points of common tangency) is not accessible. Any value of ϕ between the two points of common tangency is then achieved not by a homogeneous single phase, but by an appropriately weighted combination of the two coexisting states.

As we systematically lower the temperature (by increasing the control parameter $\beta\chi$), the shape of the free energy $f(\phi)$ varies from a simple convex curve, to become increasingly flat at the midpoint $\phi = 1/2$. Beyond $\beta\chi = 2$, the curve develops a pair of minima displaced just to either side of $\phi = 1/2$, which move progressively outward as $\beta\chi$ increases.

By plotting the ϕ values of the coexisting phases as a function of $\beta\chi$, we obtain a coexistence curve or “phase envelope”, which defines the region of two-phase coexistence for the symmetric binary mixture. (Here we plot $\beta\chi$ for theoretical simplicity; for correspondence with more usual

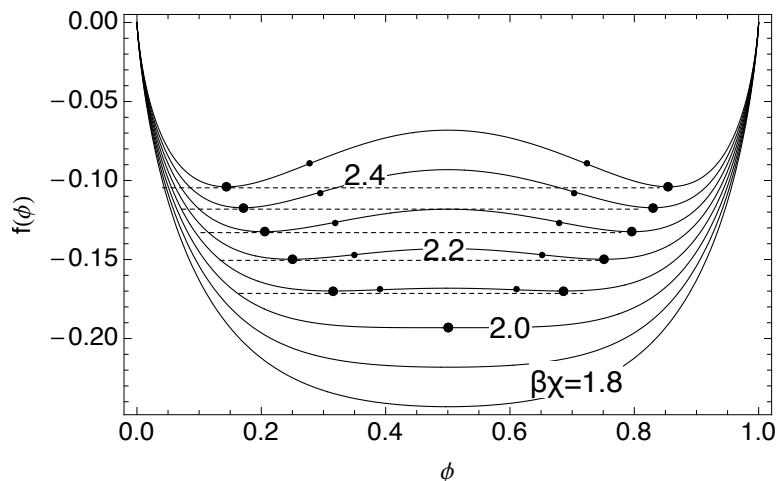


Figure 6.5: Bragg-Williams free energy per site $f(\phi)$, for indicated values of $\beta\chi$. Dashed lines are common tangents between coexisting phases. Smaller points are limits of metastability (discussed next section).

experimental plots we would invert this axis and plot $1/(\beta\chi)$, which is proportional to Kelvin temperature; this would invert the parabolic shape of the coexistence curve.)

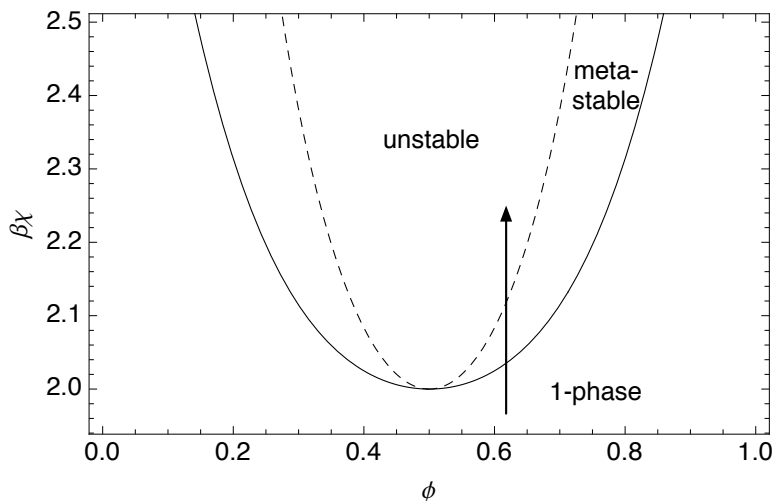


Figure 6.6: Coexistence curve (solid) and limit of metastability or “spinodal” curve (dashed), for the Bragg-Williams free energy.

6.3.2 Stability and metastability

Now suppose we have a symmetric binary mixture with a specified fraction ϕ of species A, initially at sufficiently high temperature that the system is miscible. The function $f_m(\phi)$ is convex (everywhere concave up); for whatever value of concentration ϕ we specify, there is some corresponding field value h that gives a single phase tangent.

Suppose the fixed value of ϕ is A-rich, somewhere slightly to the right of $\phi = 1/2$. Now consider what happens when we “quench” the system, i.e., lower the temperature suddenly to a temperature below T_c . If we lower the temperature enough, the composition ϕ will fall into the region of two-phase coexistence. Then the equilibrium state with average composition ϕ is a mixture of the two coexisting states ϕ_0 and ϕ_1 . The fractions f_0 and $f_1 = 1 - f_0$ of the two phases are determined by the “lever rule”,

$$f_0\phi_0 + f_1\phi_1 = \phi \quad (6.34)$$

However, the kinetic pathway for our homogeneous initial state to reach the equilibrium state of coexisting phases is very different, depending on whether or not the quenched free energy curve $f(\phi)$ is concave up or down at the initial composition ϕ .

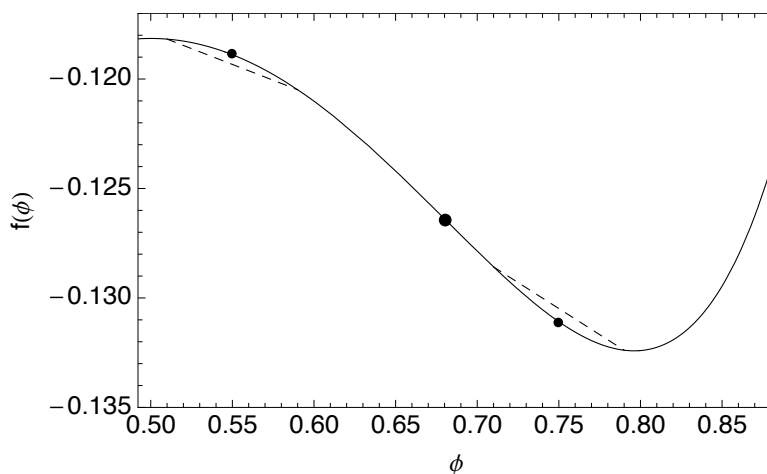


Figure 6.7: Closeup of free energy curve for $\beta\chi = 2.3$; $f(\phi)$ has inflection point (dot) at $\phi = 0.68$ — a point on the spinodal curve. $f(\phi)$ to left (right) of $\phi = 0.68$ is concave down (up), thus unstable (stable).

In Fig. 6.7, the free energy $f(\phi)$ below T_c has an inflection point at $\phi = 0.68$. Suppose first that our initial composition lies to the right of this point, but to the left of the right-hand coexisting phase (at the minimum, $\phi = 0.8$ or so). Then, $f(\phi)$ is concave up at the value of ϕ for our single phase. In this case, our homogeneous initial phase remains locally stable, in the sense that small variations of the species fraction away from the prescribed value would lead to an increase in the free energy. Our initial phase is *metastable*. For example, if we had a system which was a 50-50 mixture of ϕ values symmetrically slightly larger and smaller than $\phi = 0.75$, the free energy would by the lever rule correspond to the midpoint of the line segment connecting the two ϕ values (midpoint of right-hand dashed line in Fig. 6.7), which lies above the curve.

If our initial composition lies instead to the left of the inflection point, $f(\phi)$ is concave down at the value of ϕ for our single phase. Then, even a tiny variation in local species concentration, for example replacing a uniform ϕ by a smooth sinusoid $\phi + \delta\phi \sin(kx)$, leads to a lowering of the free energy. This is because nearby values of ϕ , say $\phi \pm \delta\phi$, give rise to a lower average value of f than the uniform $f(\phi)$. Our single phase is now *unstable* to tiny perturbations. (As an example, make the same construction as before, but now around $\phi = 0.55$; the free energy is the midpoint of the left-hand dashed line in Fig. 6.7, which lies below the curve.)

The spinodal is the locus of inflection points of the free energy curve, as the temperature (here $\beta\chi$) is varied. The spinodal composition ϕ_s thus satisfies $f''(\phi_s; \beta) = 0$. For the simple Bragg-

Williams free energy, we can compute the second derivative explicitly, to find

$$0 = -2\beta\chi + \frac{1}{\phi_s} + \frac{1}{1 - \phi_s} \quad (6.35)$$

Anticipating a result symmetric about $\phi_s = 1/2$, we write $\phi_s = 1/2 + \delta\phi_s$, and combine the two fractions to obtain

$$\beta\chi = \frac{2}{1 - 4\delta\phi_s^2} \quad (6.36)$$

Thus the spinodal temperature $1/\beta_s$ as a function of ϕ is for this model a parabola,

$$1/(\beta_s\chi) = 1/2 - 2(\phi - 1/2)^2 \quad (6.37)$$

For an initial composition somewhere away from the critical composition (here $\phi_c = 1/2$), if we cool slowly (thereby increasing $\beta\chi$) from the one-phase region, our initial homogeneous phase first crosses the phase boundary, thereby passing into the metastable region, and then crosses the spinodal, passing into the unstable region. (See Fig. [6.6](#).)

In the laboratory, single phases brought by a temperature quench into the metastable region may persist for a considerable time, until tiny droplets of the minority phase form (nucleate). After droplets of the minority phase of sufficient size are formed, they can grow by diffusion of the minority species towards the droplets, in a process called ‘‘Ostwald ripening’’, whereby equilibrium coexistence is ultimately achieved (see Section [9.4](#) below for a more detailed account of nucleation and ripening).

Whereas, for a single phase quenched into the spinodal region, even tiny concentration fluctuations present in equilibrium in the single stable phase can grow immediately, without nucleating a minority phase. This process is called ‘‘spinodal decomposition’’. The tiny concentration fluctuations grow in amplitude, quickly saturating at concentrations corresponding to the coexisting phases. Then the ‘‘spinodal pattern’’ of local regions of the two coexisting phases slowly ‘‘coarsens’’, with a steadily increasing characteristic size for the A-rich and B-rich regions, as the two species diffuse and flow to more fully phase separate (see Section [9.2](#) below for a more detailed account of this coarsening process.)

6.3.3 Experimental coexistence curves

The simple Bragg-Williams free energy gives qualitatively reasonable predictions for the behavior of a binary fluid mixture. The model leads to a critical point at $\phi = 1/2$ and $\beta_c\chi = 2$, with a parabola-shaped coexistence curve and a parabolic spinodal.

However, a closer examination of experimental data for a typical binary fluid mixture reveals that while these predictions are qualitatively reasonable, they do not agree well with the shape of experimental coexistence curves. Fig. [6.8](#) displays the coexistence curve for a binary mixture of cyclohexane and methanol.

It is apparent that the coexistence curve is much flatter than a parabola; the dashed curve is an attempt to fit a parabola to the data. The solid curve is a fit to the data assuming a form $T(\phi) = T_c - a|\phi - \phi_c|^b$, with the exponent b slightly greater than 3 (3.063).

It turns out that this qualitative discrepancy in the shape of the coexistence curve predicted by mean field theory and observed experimentally, is echoed in discrepancies in predictions for other thermodynamic quantities such as the heat capacity and isothermal compressibility in the vicinity of the critical point. We shall discuss the mean-field predictions for these quantities in the next chapter.

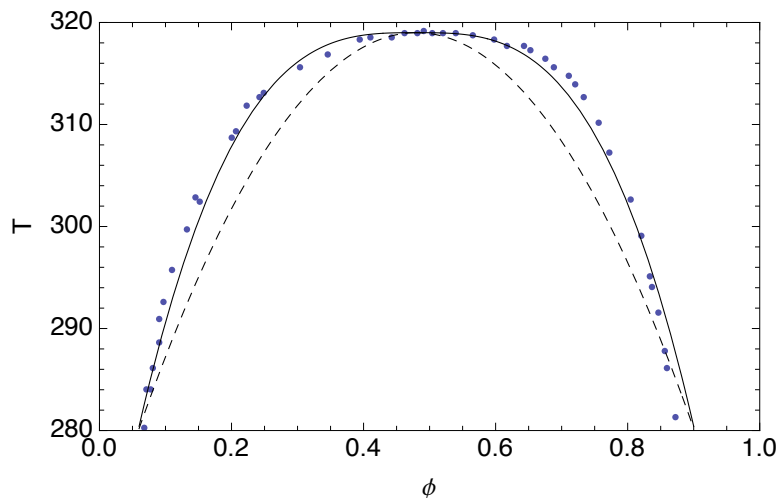


Figure 6.8: Coexistence curve for cyclohexane-methanol. Solid line: fit, of the form $T_c - a|\phi - \phi_c|^{1/\beta}$, with $\beta = 0.3265$ (3d Ising critical exponent). Dashed line: similar fit, but with $\beta = 1/2$ (mean field exponent).

For now, we observe that while mean-field theories are simple and convenient, and capture much of the qualitative behavior of the systems they describe, they cannot be relied upon for quantitatively accurate descriptions near the critical point. Furthermore, it turns out that “near the critical point” for binary mixtures actually means most of the interesting shape of the coexistence curve. Fig. 6.8 makes clear that a parabola is not a good description of the coexistence curve even for temperatures far enough below the critical point that the coexisting phases are quite well separated (10 and 90 percent compositions, say).

The origin of these discrepancies is the random mixing approximation itself, which works well at high temperatures, when configurational entropy is much more important than repulsive energy, but is progressively worse as we cool a system towards the critical point and ultimate phase separation. As we cool, the location of A and B molecules becomes more correlated, with progressively larger A-rich and B-rich patches appearing in typical system configurations. Because the error in the mean-field approximation depends on the distance to the critical point $T - T_c$, it is not surprising that the approximation fails to capture the experimentally observed dependence of quantities on T near T_c , such as the volume fractions $\phi_1(T)$ and $\phi_2(T)$ of coexisting phases.

The qualitative discrepancies between mean-field theory and experiment are the reason for the many largely phenomenological attempts to construct more accurate equations of state for simple fluids and fluid mixtures, which play an important role in practical calculations of phase behavior in chemical engineering and related disciplines.

6.4 Flory-Huggins models

Placing molecules on a regular lattice inevitably involves some compromises. Difficulties arise for example when we treat a binary mixture of molecules of somewhat different sizes: how do we choose the lattice size, and what do we do about the unpleasantly under- or overfilled lattice sites? Also, many molecules are not very well represented as roughly round; to place a long thin molecule or a plate-shaped molecule on a lattice, the molecule must occupy more than one lattice site.

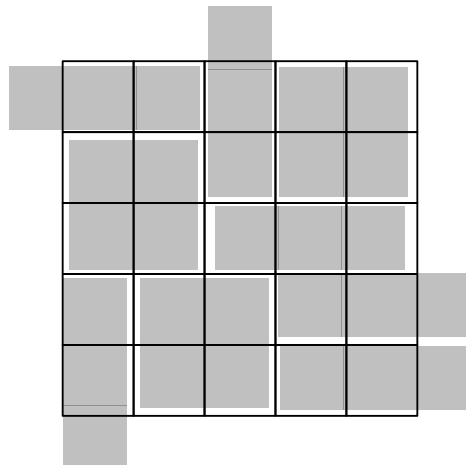


Figure 6.9: Rod-shaped and plate-shaped molecules on a lattice.

One important case that can be handled gracefully, is that of polymer-solvent or polymer-polymer mixtures. On a lattice, we may hope to represent the polymer as a sequence of moieties (“beads”) of about the same size as the solvent molecules (which we hope are reasonably round, and will thus fit in a single lattice site). The polymer will then fill a contiguous sequence of lattice sites.

We seek an extension of the simple random-mixing estimates of the interaction energy and configurational entropy, to the case of polymer-solvent and polymer-polymer mixtures. This extension was provided by Flory, and results in the Flory-Huggins free energy, which we describe in the next sections.

6.4.1 Polymer solutions

Consider a mixture of n_A polymer molecules each consisting of N_A monomers, together with n_B solvent molecules, on a lattice of N total sites. Each monomer and each solvent molecule occupies a single lattice site. We would like to make random-mixing estimates for the average interaction energy per site E/N and the configurational entropy per site S/N .

Estimating the interaction energy assuming completely random mixing is easy; in fact, the simplest answer is the same as we wrote in Eq. (6.4). (This expression neglects even the connectivity of each individual polymer, which guarantees that two of the z nearest neighbors of each monomer will also be monomers.)

It is more difficult to estimate the configurational entropy, because we cannot as before simply count the number of ways of placing the monomers on the lattice, making each choice independently from among the remaining open sites.

Flory introduced the following approximate scheme for counting the number of configurations Ω , as follows. First, place the n_B identical solvent molecules on the lattice; the number of ways to do this is

$$\Omega_B = \binom{N}{n_B} = \frac{N!}{n_B!(N - n_B)!} \quad (6.38)$$

Now, we estimate the number of ways to place the n_A polymers on the remaining open sites of the lattice. We proceed by randomly choosing a lattice site for one end of each of the n_A chains, without worrying about whether the site is filled or not. Then, we generate a random configuration for each chain, starting from its free end, again without worrying about whether the needed lattice sites are open. For each chain, there are z^{N_A} possible configurations. The total number of possible configurations for the A chains is then

$$\Omega_A = \frac{N^{n_A} (z^{N_A})^{n_A}}{n_A!} \quad (6.39)$$

where the factor of $n_A!$ accounts for indistinguishability of the A chains.

Finally, we estimate the (rather small!) chance that the configuration we generated actually works, i.e., that all the necessary sites were unfilled before we placed the A chains. We have $n_A N_A$ monomers to place, and an equal number of lattice sites to hold them; but we placed the monomers blindly. So the probability that the first site we choose is open is $(N - n_B)/N$ (because n_B sites are filled already), the probability that the second site is open is $(N - n_B - 1)/N$, and so forth down to $1/N$.

We need *all* of the sites to be open for the configuration to be valid; this happens with (very small!) probability

$$P = \frac{(N - n_B)!}{N^{n_A N_A}} \quad (6.40)$$

(Note that this expression for P is an estimate, not exact, because it neglects the correlations in where we place monomers that result from the connectivity of the chains.)

The number of valid configurations is then the total number of configurations $\Omega_A \Omega_B$, times the probability P that a configuration is valid:

$$\Omega = \frac{N! N^{n_A} z^{N_A n_A}}{n_A! n_B! N^{n_A N_A}} \quad (6.41)$$

Evaluating S/k as $\log \Omega$, using the Stirling approximation, gives after some algebra

$$S/(kN) = -(n_A/N) \log(n_A/N) - (n_B/N) \log(n_B/N) + (n_A/N)(1 + N_A \log z) + (n_B/N) \quad (6.42)$$

The last two terms are linear in the number of A chains and B solvent molecules, and can be absorbed by a redefinition of the zero of chemical potential for each species.

(The factor $(N_A \log z)$ is an estimate of the conformational entropy of each A chain, which chooses among z directions to take each step in its random walk conformations. In our approximation, this conformational entropy is independent of the translational entropy, i.e., where on the lattice the chain ends were located.)

Writing ϕ as the site fraction of A monomers, we have ϕ equal to $n_A N_A / N$, and hence

$$S/(kN) = -(\phi/N_A) \log(\phi/N_A) - (1 - \phi) \log(1 - \phi) \quad (6.43)$$

Combined with the random mixing estimate of the repulsive energy, we arrive at the Flory-Huggins free energy per site,

$$F/N = \chi\phi(1 - \phi) + kT [(\phi/N_A) \log(\phi/N_A) + (1 - \phi) \log(1 - \phi)] \quad (6.44)$$

Evidently this function is no longer symmetric under exchange of ϕ and $1 - \phi$, because monomers and polymers are not structurally identical entities. The entropy term is suggestive of the sum of two ideal gases, one of polymer ends (or centers of mass), and one of solvent particles.

The Flory-Huggins free energy reduces to the Bragg-Williams result for $N_A = 1$ (the polymer is a single A monomer, the same size as a B solvent molecule). However, the Flory-Huggins free energy and the behavior that derives from it are not symmetric under interchange of A and B, for N_A greater than unity.

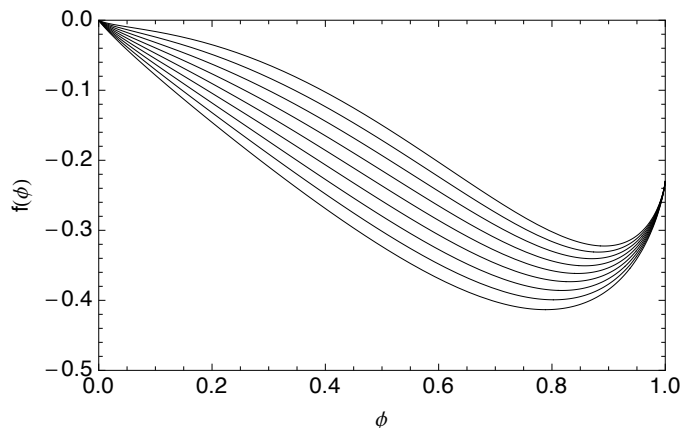


Figure 6.10: Flory-Huggins free energy per site $f(\phi)$ for $N = 10$, and $\beta\chi$ values equal to 0.8, 0.9, 1.0, ... 1.6 times the critical value.

For polymers ($N_A \gg 1$), the phase diagram that results from Eq. (6.44) is quite asymmetric. Below the critical point, the solvent-rich phase tends to be extremely dilute in polymer, while the polymer-rich phase contains a decent amount of solvent. This is because the translational entropy per monomer is extremely small for polymers, so there is little entropy gain per monomer from dragging polymers into the unfavorable solvent. Whereas, the translational entropy per solvent molecule is enough of an incentive for at least some solvent molecules to enter the polymer-rich phase despite the repulsive polymer-solvent interaction.

6.4.2 Origin of χ

In writing Eq. (6.2) for the interaction energy of binary mixtures on a lattice, we simply assumed that the local energetic interaction took the form of a penalty for unlike species occupying adjacent sites. But really, all molecules in a nonpolar liquid interact attractively with each other by van der Waals or dispersive interactions, even when the molecules are dissimilar. The r^{-6} attractive tail of the Lennard-Jones potential is a representation of this attraction, which arises from the interaction of quantum-mechanical dipole fluctuations on one molecule and the dipole on a second molecule induced by the dipole field of the first molecule.

Here, we briefly consider how a single repulsive χ parameter results from competing attractive interactions between AA, AB, and BB pairs of molecules. In a lattice model, we may approximate the Lennard-Jones interaction as being sufficiently short-ranged to only involve nearest-neighbors pairs of molecules, with an attractive energy ϵ_{AA} between an adjacent pair of A molecules, ϵ_{AB} between an A and an adjacent B, and ϵ_{BB} between a B pair.

Then, in a random mixing approximation, the energy per site would be

$$E/N = -(z/2) (\epsilon_{AA}\phi_A^2 + 2\epsilon_{AB}\phi_A\phi_B + \epsilon_{BB}\phi_B^2) \quad (6.45)$$

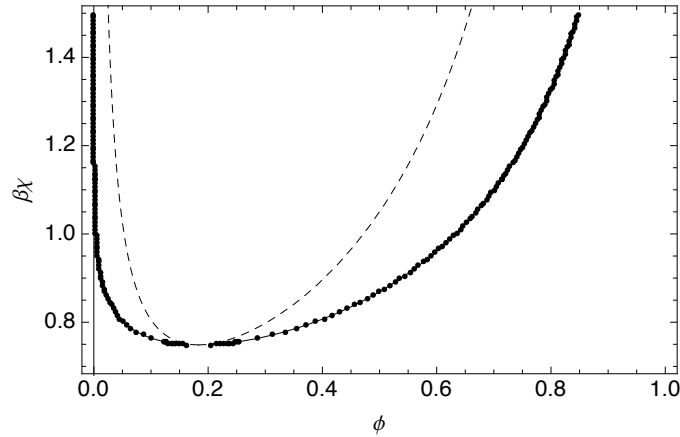


Figure 6.11: Flory-Huggins phase diagram, for $N_A = 20$. Connected points, coexistence curve; dashed line, spinodal.

To write the above, we observe that there are $z/2$ bonds per site in the lattice, and that each bond will connect two A molecules with probability ϕ_A^2 (the probability that both molecules are A), will connect an A and a B with probability $2\phi_A\phi_B$ (we could have either AB or BA on the bond), and so forth. The overall minus sign denotes attractive interactions (we take the signs of the various ϵ values to be positive for simplicity).

In writing the above equation, we have implicitly taken the zero of energy to be a reference state of isolated A and B molecules, with no interactions whatsoever. A more convenient choice for the reference state turns out to be a system completely demixed into pure A and pure B regions, for which the energy per site would be

$$E_0/N = -(z/2)(\epsilon_{AA}\phi_A + \epsilon_{BB}\phi_B) \quad (6.46)$$

Taking the difference $\Delta E = E - E_0$ and rearranging, we find

$$\Delta E/N = (z/2)(\epsilon_{AA} + \epsilon_{BB} - 2\epsilon_{AB})\phi_A\phi_B \quad (6.47)$$

which allows us to identify

$$\chi = (1/2)(\epsilon_{AA} + \epsilon_{BB} - 2\epsilon_{AB}) \quad (6.48)$$

We see that χ is positive if the attraction between like pairs of molecules is greater on average than the attraction between an unlike pair of A and B, even if all interactions are attractive.

For dispersive interactions, it turns out that $\epsilon_{\alpha\beta}$ for interaction between molecules of type α and type β can be written as

$$\epsilon_{\alpha\beta} = \delta_\alpha\delta_\beta \quad (6.49)$$

The physical origin of this simplification is that the same quantity governing the strength of quantum-mechanical dipole fluctuations of a molecule also governs the polarizability of that molecule by an external field (such as the dipole field of another molecule).

Writing the various ϵ parameters in this way, we have finally

$$\chi = (1/2)(\delta_A - \delta_B)^2 \quad (6.50)$$

which is evidently positive, for any values of δ_A and δ_B . If the interactions between molecules in a binary mixture are purely dispersive, then the net interaction is always repulsive, and can only be made zero by arranging for the two species to have matched molecular polarizabilities.

However, not all interactions between monomers are the result of dispersive interactions. An important origin of local interactions between certain classes of polar monomers are hydrogen-bonding (H-bonding) interactions. A simple view of H-bonding interactions is as follows. Some monomers have a localized region on their surface that is somewhat positively charged; most often, this is a relatively acidic proton on some monomer, partly stripped of its electronic cloud by being bonded directly or indirectly to an electron-withdrawing atom or group.

Other monomers may display on their surface a localized region that is somewhat negatively charged; this may be for example the “lone pair” of electrons on an ether oxygen, or the slightly negative electron cloud on a chlorine bonded to a carbon. These oppositely charged surface groups can then be electrostatically attracted to each other, in much the same way as the slightly positively charged hydrogen atom is attracted to the lone pair on the oxygen in an H-bond in water.

H-bonds can be either strong or weak depending on how large, localized, and accessible are the charges of the H-bond “acceptor” (positive moiety) and “donor” (negative moiety). For our present purposes, the important feature of H-bonds between monomers A and B is that their strength can be roughly represented as the product of the “donor strength” δ and the “acceptor strength” α . Each monomer can be represented as having both a donor strength and an acceptor strength. The interaction energy ϵ_{AB} between monomers A and B can then be written

$$\epsilon_{AB} = \delta_A \alpha_B + \delta_B \alpha_A \quad (6.51)$$

because either monomer can in principle play the role of donor or acceptor, depending on the orientations of the monomers (not explicitly represented in a simple lattice model).

Substituting this result into Eq. (6.48) for χ , results in

$$\chi = (\delta_A - \delta_B)(\alpha_A - \alpha_B) \quad (6.52)$$

Unlike Eq. (6.50) for χ resulting from dispersive interactions, the above expression is not necessarily positive. In fact, we can arrange for χ arising from H-bonding to be negative and thus attractive, by selecting a pair of monomers such that one is a strong H-bond acceptor but a weak donor, and the other is a strong donor but a weak acceptor. In such a case, strong H-bonds can only form when the polymers are mixed. This strategy is an important practical technique for designing miscible polymer blends.

6.4.3 Polymer blends

It is straightforward to generalize the counting argument of Section 6.4.1 above to the case in which both species B is also polymeric, with n_B chains present each with N_B monomers. We simply use the same approximate technique to count the number of ways to place the B chains on the lattice, that we used for the A chains previously.

Thus we replace the counting factor Ω_B with

$$\Omega_B = \frac{N^{n_B} (z^{N_B})^{n_B}}{n_B!} \quad (6.53)$$

identical in form to the Ω_A factor previously. Likewise, we amend the success probability factor P to read

$$P = \frac{N!}{N^{n_A} N_A N^{n_B} N_B} \quad (6.54)$$

Assembling the factors Ω_A , Ω_B , and P results in

$$\Omega = \frac{N! N^{n_A} z^{N_A n_A} N^{n_B} z^{N_B n_B}}{n_A! n_B! N^{n_A} N_A N^{n_B} N_B} \quad (6.55)$$

Evaluating S/k as $\log \Omega$ using the Stirling approximation, gives after some algebra

$$\begin{aligned} S/(kN) &= -(n_A/N) \log(n_A/N) - (n_B/N) \log(n_B/N) \\ &+ (n_A/N)(1 + N_A \log z) + (n_B/N)(1 + N_A \log z) \end{aligned} \quad (6.56)$$

Writing S in terms of the monomer fractions $\phi_A = n_A N_A/N$ and ϕ_B likewise, and dropping linear terms as previously, results in

$$S/(kN) = -(\phi_A/N_A) \log(\phi_A/N_A) - (\phi_B/N_B) \log(\phi_B/N_B) \quad (6.57)$$

For large N_A and N_B , in the approximation we have made, the polymer blend looks essentially like a mixture of two ideal gases of chain ends, with the implicit assumption that the conformational entropy of the chains is unaffected by where the chains are placed. (This is actually a rather good assumption for polymer blends, as we shall explain below.)

The full Flory-Huggins free energy per site for the polymer blend is then

$$F/N = \chi \phi_A \phi_B + kT [(\phi_A/N_A) \log(\phi_A/N_A) + (\phi_B/N_B) \log(\phi_B/N_B)] \quad (6.58)$$

For the particular case of polymers of equal length ($N_A = N_B$), we once again have symmetry under interchange of A and B species.

Indeed, the Flory-Huggins free energy for $N_A = N_B = N$ looks almost the same as the Bragg-Williams free energy, if we dispense with some linear terms arising from the logs in the entropy (which, as we remarked earlier, only serve to shift the chemical potential):

$$F/N = \chi \phi(1 - \phi) + kT/N [\phi \log(\phi) + (1 - \phi) \log(1 - \phi)] \quad (6.59)$$

The important difference between the above expression and that for a binary mixture of monomers is that the entropy is multiplied by a factor of $1/N$, since only each chain (rather than each monomer) has an independent translational degree of freedom. As a result, a much smaller value of χ suffices to drive phase separation; instead of the critical point being located at $\beta\chi = 2$ (and $\phi = 1/2$), the critical temperature now satisfies $\beta\chi = 2/N$.

Physically, we say that polymers are much more susceptible to demixing, because even very weak repulsive interactions per monomer (χ of order $2kT/N$) suffices to overcome the very weak translational entropy (of order kT per *chain*). All polymers have dispersive interactions, which we have argued generically lead to repulsive (positive) χ parameters, and can only be made small by matching the molecular polarizabilities of the two species. This makes it very difficult to design miscible blends of long nonpolar polymers (large N).

But, as we observed at the end of Section [6.4.2](#), interactions such as hydrogen bonding are qualitatively different from dispersive attractions in that the simple rule is not “like prefers like”, but “opposites attract”. This suggests a general strategy for designing miscible polymer blends, which is to arrange for one monomeric species to be a good hydrogen bond donor but a poor acceptor, and the other species to be a good acceptor but poor donor, so that favorable hydrogen bonds can only be formed by mixing the two species. Then χ can be negative, favoring mixing.